“En el campo hubo de todo: sequía, caracol, fiebre aftosa.”

Isabel Allende

in La casa de los espíritus

0. Introduction

0.1   Surface Plasmon Resonance

0.1.1   The physical phenomenon[1-6]

When a beam of light propagating through a first medium of higher refractive index, n_1 (*e.g.* a glass or quartz prism) meets an interface with a second medium of lower refractive index, n_2 (*e.g.* an aqueous solution), then it will be totally internally reflected for all incident angles greater than a critical angle θ_c:

$$\theta_c = \sin^{-1}(n_2/n_1) \tag{0.1}$$

where θ is the angle between the incident beam and the axis normal to the plane of the interface. This phenomenon is known as *total internal reflection* (TIR)[4]. Despite being totally reflected, the incident beam establishes an electromagnetic field that penetrates a small distance into the second medium, where it propagates parallel to the plane of the interface (Fig.
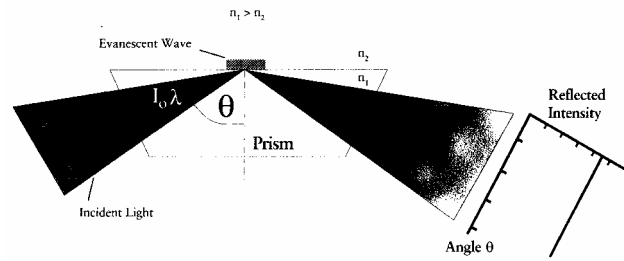

Figure 0. 1 Schematic view of the total internal reflection (TIR) phenomenon[3].

0.1). This electromagnetic field is called the *evanescent wave*. The intensity of the evanescent electric field, $I(z)$, decays exponentially with perpendicular distance z from the interface:

$$I(z) = I_o e^{-z/d} \tag{0.2}$$

where d is the penetration depth for angles of incidence $\theta < \theta_c$ and light of wavelength λ_o:

$$d = (\lambda_o/4\pi)(n_1^2 \sin^2\theta - n_2^2) \tag{0.3}$$

d is independent of incident light polarisation but depends on its wavelength. The evanescent electric field intensity at $z=0$, I_o, depends both on θ and the incident beam polarisation. When the beam is polarised parallel to the plane of the interface, I_o is given by $I_o^{//}$:

$$I_o^{//} = I^{//}[4\cos^2\theta(2\sin^2\theta - n^2)]/(n^4\cos\theta + \sin^2\theta - n^2) \tag{0.4}$$

When the beam is polarised perpendicular to the plane of the interface, the field intensity at $z=0$ is equal to:

$$I_o^{\perp} = I^{\perp}(4\cos^2\theta)/(1-n^2) \qquad\qquad (0.5)$$

$I^{//}$ and $I^{\perp}$ are the intensities of the incident light beam polarised parallel or perpendicular to the interface, respectively, and $n=(n_2/n_1)<1$. Therefore, two major characteristics of the evanescent wave are worth to notice:

i) the depth of the evanescent wave is typically less than a wavelength, thus extending a few hundred nm into the dielectric (liquid phase of refractive index n_2);

ii) the evanescent field intensity, I_o, for angles a few degrees above the critical angle θ_c is several times the incident intensity, I.

When a thin metal film is inserted at the prism/dielectric interface, a new phenomenon called *surface plasmon resonance* (SPR) can occur[5]. Surface plasmons are waves of oscillating surface charge density (conducting electrons) propagating along the metal surface, at a metal (*e.g.* silver or gold)/dielectric (*e.g.* aqueous solution) interface. The field amplitude of the surface plasmon is maximal at the interface and decays evanescently, *i.e.*, perpendicularly to it, with a penetration into the dielectric of about 100-200 nm. Due to high loss in the metal, the surface plasmon wave propagates with high attenuation in the visible and the near-infrared spectral regions. The distribution of the electromagnetic field of a surface plasmon wave is highly asymmetric and the majority of the field is concentrated in the dielectric (Table 0.1).

Table 0.1 Major characteristics of surface plasmon waves (SPW) at the metal-water interface[6].

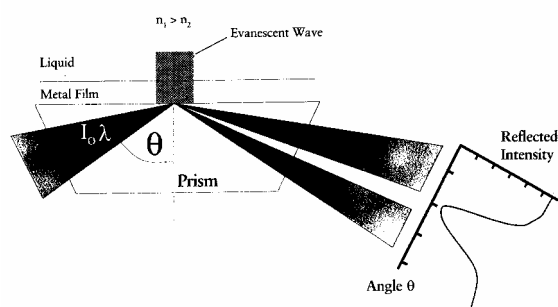| Metal layer supporting SPW	Silver		Gold	
Wavelength (nm)	630	850	630	850
Propagation length(μm)	19	57	3	24
Penetration depth into metal (nm)	24	23	29	25
Penetration depth into dielectric (nm)	219	443	162	400
Concentration of field in dielectric (%)	90	95	85	94

Figure 0. 2 Schematic view of the surface plasmon resonance (SPR) phenomenon[3].

Surface plasmons cannot be directly excited (resonate) by light, since the frequency and wave vector requirements cannot be simultaneously matched. Nevertheless, indirect excitation can be achieved by an evanescent wave created by the internal reflection of a *p*-polarised incident beam at the metal-coated surface of the prism.

This excitation, or resonance, occurs only at a well-defined angle of incidence, θ_{sp}, given by:

$$\theta_{sp} = \sin^{-1}(k_{sp}/n_g k_o) \qquad\qquad (0.6)$$

where n_g is the refractive index of the prism, λ is the wavelength of the incident light in the vacuum, k_{sp} is the wave vector of the surface plasmon and k_o is the wave vector of the light in the vacuum $k_o = 2\pi/\lambda$. When the resonance condition is fulfilled, energy from the incident light is transferred to the non-radiative surface plasmon and converted to heat. This energy loss is recognised by a sharp minimum ($\leq 1°$ at half-width) in the angle-dependent reflectance (Fig. 0.2).

0.1.2   SPR optical sensors and their applications[1-31]

The phase matching, *i.e.*, the resonance angle θ_{sp}, is very sensitive to changes in wavelength, metal thickness and refractive indices of the prism (n_1) and of the dielectric (n_2). However, if the first three factors are all kept constant, θ_{sp} will depend only on the refractive index (*i.e.*, on the dielectric constant) of the dielectric (n_2). A change in the dielectric refractive index very close to the metal surface will originate a change in the resonance angle θ_{sp}, which is the principle of SPR sensing.

Considering the unique characteristics of SPR detection, it is possible to design SPR sensors that, under the proper geometries, allow the sensing of physical, chemical or biochemical phenomena which give rise to changes in the optical properties of the solution (dielectric) very close to the metal surface.

Generally, an SPR optical sensor is composed of an optical system, a transducing medium inter-relating the optical and the reagent domains, and an electronic system controlling the optoelectronic devices and allowing data processing. The transducing unit transforms changes in the refractive index, determined by continuously monitoring the SPR angle, into changes in the quantity of interest. Measurement of the angular dependence of reflectance from an SPR sensor surface requires a monochromatic light source, such as a small gas laser (HeNe at 633 nm) or a solid state diode in the far red. The optical pathway can include elements for polarisation in the incident plane (*p*-polarisation), attenuation, spatial filtering and shaping the beam to a convergent wedge focused at the SPR surface of a hemicylindrical glass prism (Fig. 0.3).
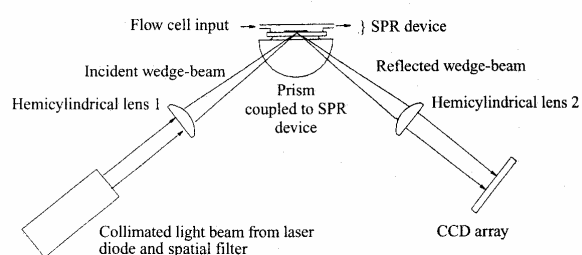

Figure 0. 3 Optical apparatus for the measurement of the angular dependence of resonance[1].

SPR sensing has a wide variety of applications. Measurement of *physical* properties such as displacement and angular position using SPR sensors has been described[7,8]. Exploitation of physical phenomena occurring in optical transducing materials allowed the development of specific SPR sensors, such as humidity detectors using humidity-induced refractive index changes in porous thin layers and polymers[9]. The thermooptic effect in hydrogenated amorphous silicon has also been used to create an SPR-based temperature sensor[10].

Chemical SPR sensors are based on the measurement of SPR variations due to adsorption or chemical reaction of an analyte within a transducing medium which causes changes in its optical properties. Examples of chemical applications of SPR due to analyte adsorption include: monitoring of hydrocarbons, aldehydes and alcohols adsorbing on polyethyleneglycol films[11]; monitoring of chlorinated hydrocarbons adsorbing on polyfluoroalkylsiloxane[12]; detection of aromatic hydrocarbons adsorbing on Teflon film[13]. SPR devices using palladium are effective in the detection of molecular hydrogen[14]; also, chemisorption of NO_2 on gold has been used for NO_2 detection[15]. Copper and nickel phtalocyanine films have been used for SPR detection of toluene[16], while bromo-cresol purple films have been employed for the detection of NH_3 vapours[17]. SPR detection of Cu and Pb ions was also made possible by combination with anodic stripping voltammetry[18].
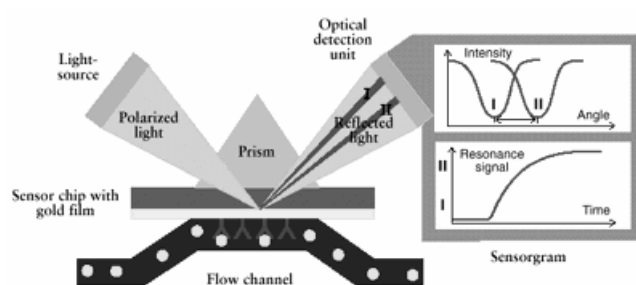

Figure 0. 4 SPR detection caused by biospecific binding of ligand in solution to an immobilised receptor[22].

Affinity SPR biosensors are the most widely employed, where SPR, as a surface-oriented method, allows real-time analysis of biospecific interactions without the use of labelled biomolecules. The SPR biosensor technology has been commercialised and has become a central tool for characterising and quantifying biomolecular interactions.

Since the first demonstration, in 1983, of the viability of SPR biosensing[19], SPR detection of biospecific interactions was developed until the appearance, in 1994, of the first analysis methods for surveying biomolecular interactions in real-time[3]. These methods have been improved for the study of kinetic and thermodynamic constants of those interactions. Generally, SPR biosensing relies on the immobilisation of the biological receptor at the chemically modified gold surface, which is in contact with a buffer solution[20]. Upon addition of a specific ligand to the solution, binding occurs close to the gold surface, allowing for SPR detection due to mass increase, and consequent change in the refractive index in this region (Fig. 0.4)[21]. The shift in the resonance angle acts as a mass detector and the continuous angular interrogation in the SPR-sensing device allows for the real-time monitoring of binding, providing kinetic data on the biospecific interaction. Prism-based SPR biosensors using angular interrogation have been employed in studies of antigen-antibody[23-26], protein-protein[27,28], protein-DNA interactions[29]and epitope mapping[30,31]. Many other biomolecular studies are presently among the applications of SPR biosensing, which has become a part of modern analytical methods.

0.2   Real-Time Biospecific Interaction Analysis

The use of optical biosensors for interaction analysis has made it possible to obtain affinity and kinetic data for a large number of protein-protein, protein-peptide and protein-DNA systems. Biosensor AB (Uppsala, Sweden) is undoubtedly the biosensor market leader, since it launched, in late 1990, the first commercial SPR-based instrument, BIAcore[32-36].

0.2.1   The BIAcore technology[3,20-22,37,38]

BIAcore uses SPR to investigate biospecific interactions at the surface of a sensor chip. One of the components in the interaction is immobilised on the sensor chip surface and the other flows over the surface free in solution. As the interaction proceeds, the concentration (mass) of analyte in the surface layer changes, giving an SPR response which can be followed in real-time in the form of a *sensorgram* (Fig. 0.5). The instrument consists of a processing unit, reagents for ligand immobilisation, exchangeable sensor chips and a personal computer for control and evaluation. The processing unit contains the SPR detector and an integrated microfluidic cartridge that, together with an autosampler, controls the delivery of sample plugs into a transport buffer which flows continuously over the sensor chip surface (Fig. 0.6). All the injection and detection systems are thermostatically

Figure 0. 5 Sensorgram: monitoring the SPR response in terms of binding to receptor[22].
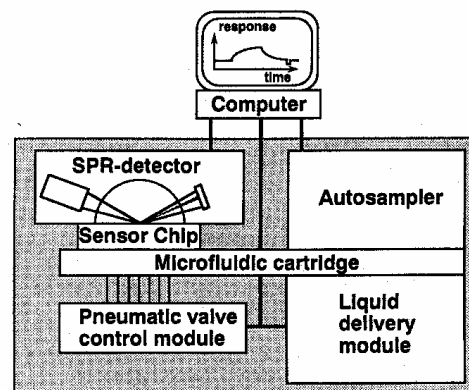
Figure 0. 6 Scheme of the BIAcore instrument[21].

controlled so that BIAcore measurements are carried out at constant temperature. The light source in BIAcore is a near-infrared light-emitting diode (LED) and light is focused on the gold film as a wedge-shaped beam giving a fixed range of incident angles. The SPR response is monitored by a fixed array of light-sensitive diodes covering the whole wedge of reflected light. Reagents, buffers and samples are delivered to the sensor chip surface through a liquid handling system composed by three main parts: the pumps, the sample injector and the integrated fluidic cartridge (IFC). One of the pumps is used to maintain the continuous flow over the surface, while the other is used for injection of samples and reagents *via* the autosampler (sample injector). This autosampler is programmed to take defined volumes of liquid from specified sample positions to either other sample positions or to the IFC injection port.
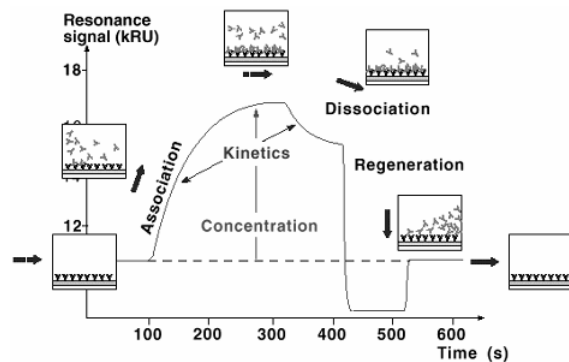
0.2.2   Ligand immobilisation[3,20-22,37,39,40]

Sensor chip architecture

 The sensor chip is a glass slide onto which a 50-nm thick gold film has been deposited. Immobilisation by physical adsorption on gold has disadvantages, namely ligand denaturation, non-specific binding and steric hindrance. Therefore, the gold surface has been chemically modified to allow ligand covalent immobilisation[39] in order to obtain a stable ligand surface, with the possibility of repeated analyses and maximum exposure of the ligand to the solution containing the biospecific partner (Fig. 0.7).
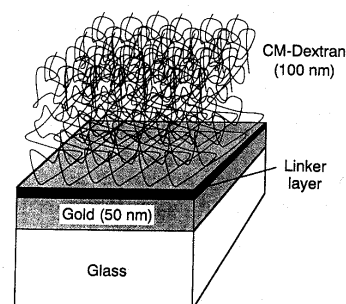

Figure 0. 7 Sensor chip CM5[21,22].

Immobilisation chemistry

Proteins are, by far, the most widely employed ligands in biospecific interaction analysis. Therefore, the development of chemistries for ligand immobilisation was based on protein chemistry, namely on the reaction between protein primary amino groups and the carboxyl groups from the carboxymethyldextran matrix to form amide bonds. Immobilisation starts by activation of the matrix COOH groups as N-hydroxysuccinimide active esters, upon reaction with N-hydroxysuccinimide (NHS) in the presence of N-ethyl-N'-(dimethylaminopropyl)carbodiimide (EDC), in water. Next, a protein solution at low ionic strength and pH below the isoelectric point is passed over the surface and protein-matrix amide bonds are formed (Fig. 0.8). The efficiency of the immobilisation step relies simultaneously on two factors:

i)   Electrostatic pre-concentration of positively charged protein in the negatively charged carboxymethyldextran matrix, and

ii)   Reaction between the protein primary amines and the matrix active esters.

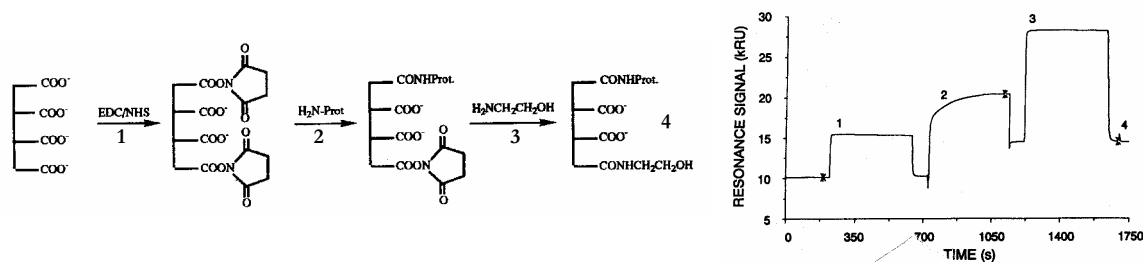**Figure 0. 8** Steps in the standard ligand immobilisation on CM5 sensor chips: **1**. COOH activation with EDC/NHS; **2**. Ligand coupling; **3**. Blocking of remaining reactive NHS-ester groups with ethanolamine; **4**. Final ligand surface[20].

Remaining active esters after protein immobilisation are converted into inactive amides *via* reaction with ethanolamine. The SPR detector continuously monitors the immobilisation steps (Fig. 0.8) and the amount of immobilised protein can be controlled either by protein concentration, reaction time or other factors such as ionic strength or pH[20]. NHS-esters are also reactive with other nucleophilic groups from the ligand, such as thiol or aldehyde groups (Fig. 0.9). Other chemical modifications based on NHS-active esters were proposed[40]:

Figure 0. 9 Ligand immobilisation based on NHS-ester activation[22].

i)   Formation of an amine derivative by reaction of the NHS-esters with ethylenediamine;

ii)   Similar preparation of a hydrazide derivative upon reaction of hydrazine with the NHS-active esters;

iii)   Obtention of a maleimide derivative adding sulfo-*m*-maleimidobenzoyl-N-hydroxysuccinimide ester (sulfo-MBS) to the amine surface prepared according to i).

Tailor-made sensor chips

The high versatility of the carboxymethyldextran matrix in sensor chip CM5 is accompanied by a very high binding capacity and low non-specific binding suitable for the majority of biospecific analyses, particularly those involving kinetic studies on low-molecular weight analytes or concentration analysis. However, the size and charge density of the matrix can be detrimental for specific studies, such as those involving high-molecular weight molecules or complex culture media. Presently, a set of sensor chips in which the dextran matrix has been tailored to suit various experimental studies is available, ranging from chips with absent (C1) or shortened (F1) dextran polymers to chips with reduced charge density (B1) in the dextran matrix. Other specific sensor chips are also available, such as a plain gold surface (J1) suitable to create new surface chemistries, a streptavidin (SA) surface to capture biotinylated ligands, a nitrilotriacetic acid (NTA) surface with capture *via* nickel chelation and a flat hydrophobic (HPA) surface for membrane biochemistry.

0.2.3   General methodology[3,21-31,37,41-54]

Binding strategies

Methods for real-time biospecific interaction analysis include single- or multi-step binding to the sensor chip surface and direct or indirect measurement of analyte. In *single-step* methods binding of one component to the immobilised ligand is measured, while in *multi-step* methods sequential binding of two or more components is monitored. When the interaction of the analyte itself with the modified sensor surface is monitored, the method is *direct* and in such case the response increases with increasing amount of analyte. *Indirect* methods rely upon measurement of a component which either:
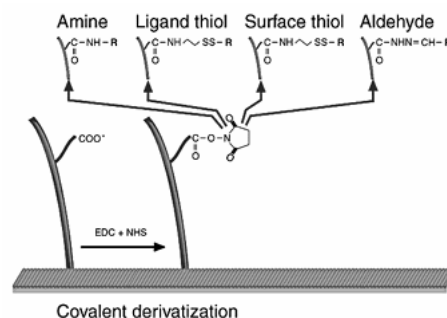
i)   interacts with analyte in solution and the remaining free concentration in solution is measured (*solution affinity*), or

ii)   competes with the analyte of interest for the same ligand binding site (*surface competition*).

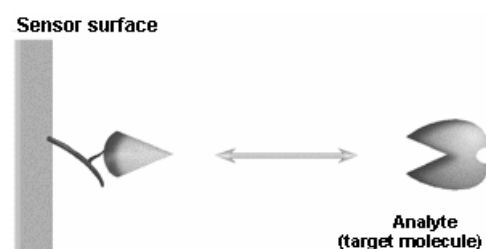In indirect methods, the response is inversely related to the amount of analyte.

Figure 0. 10 Direct single-step detection of analyte on the sensor surface[22].

Direct single-step methods (Fig. 0.10) are the simplest way to study biospecific interactions and are commonly used for *kinetic studies* and for *concentration measurement* of macromolecules at relatively high quantities (medium to large analytes above *ca.* 1 µg/ml)[23,27,28,41-45].

Direct multi-step methods are assays in which each stage in the series of binding steps is recorded in the sensorgram. A common use of these methods consists in the immobilisation of a capturing molecule (*e.g.* streptavidin, anti-immunoglobulin) that specifically binds the ligand (biotinylated molecule, immunoglobulin), which is the receptor of the target analyte (Fig. 0.11)[29,46-48]. This affinity capture allows
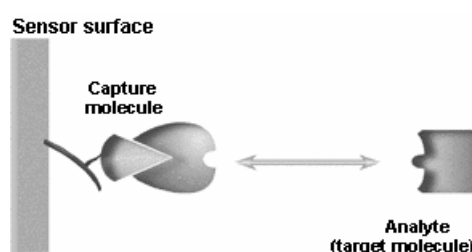

Figure 0. 11 Direct multi-step detection of analyte on the sensor surface[22].

the use of non-pure samples of ligand (*e.g.* from cell culture media) and also the oriented non-covalent immobilisation of ligand. These methods are often employed in *binding site analysis* such as epitope mapping[30,31,49]. Another application of multi-step methods is the use of a secondary molecule to enhance analyte response in sandwich assays where an analyte binds an immobilised ligand and a second macromolecule is then injected to bind the bound analyte.
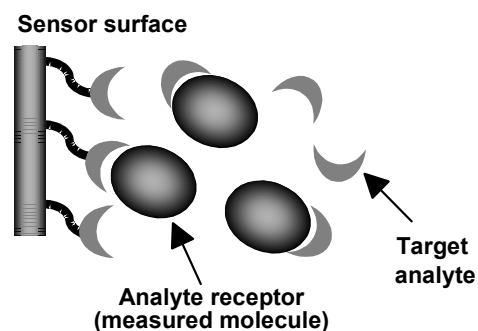

Figure 0. 12 Solution affinity studies – the target analyte is pre-equilibrated with its biospecific receptor in solution and remaining free receptor is measured on the surface.

Indirect methods are most widely employed for small analytes (molecular weight<1000 Da) in solution. Direct detection of such analytes is often difficult and these usually lack multiple independent binding sites necessary for response enhancement with sandwich techniques. In *solution affinity* experiments the analyte and a specific receptor interact in solution and, once equilibrium is reached, the remaining free receptor is determined by SPR using a sensor chip where another ligand (*e.g.* the analyte itself) is immobilised (Fig. 0.12)[24,25,50,51]. Thus, the solution affinity between analyte and receptor can be determined.

Sensor surface

Target analyte (small competitor)
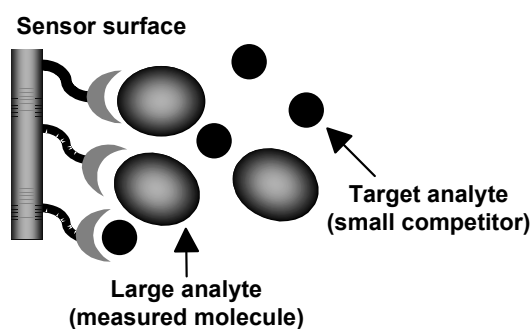
Large analyte (measured molecule)

Figure 0. 13 Surface competition between the small target analyte and the SPR-detected macromolecule.

In *surface competition* assays a high molecular weight analyte is usually employed to compete with the low molecular weight target analyte for the same ligand binding site. Since response due to small analyte binding is unappreciable, only the response from the large analyte is monitored. Therefore, the effects on the kinetics of macromolecule binding due to additions of small competing analyte can be measured and the kinetics of small analyte binding can be indirectly determined (Fig. 0.13)[52].

Surface regeneration

Regeneration of the ligand surface allows for the re-utilisation of the same biospecific surface for series of measurements, obviating the need to replicate identical surfaces. The most general regeneration methods rely on pH reduction below 2.5 using strong inorganic acids such as 10-100 mM HCl or H_3PO_4 or weaker acids such as glycine buffers. Nevertheless, ligand tolerance to acids is variable and, on the other hand, many ligand-analyte complexes may not be disrupted under acidic conditions. Therefore, regeneration procedures must be optimised and many regenerating agents other than acids (bases such as 10 mM NaOH, high ionic strength solutions such as 1M NaCl, etc.) may be found to be more effective. A systematic regeneration optimisation protocol has been recently described and successfully applied to antibody surfaces[53,54]. Stock solutions are mixtures of similar components (*e.g.* all acids, all bases, all salts, all detergents, etc.) and regeneration cocktails are different combinations of such stock solutions. Fine-tuning of regeneration cocktails may provide the answer to problems not overcome with standard regeneration methods and allow for the use of molecules that, otherwise, would not be suitable as easy-to-regenerate ligands.

0.3   *Measuring kinetics of biospecific interactions*

Characterisation of the affinities and rates of biospecific interactions is fundamental in many areas of biochemical research. Methods that measure changes in optical parameters, such as fluorescence or absorbance, can be employed for direct kinetic analysis. However, these methods require that one of the reactants is often labelled with a radioactive or fluorescent probe and thus no longer in native form. SPR detection is more general than these methods, since it is sensitive to changes in mass and no labelling is required. When analyte is injected across a ligand surface, the resulting sensorgram displays three essential phases, namely, *association* of analyte with ligand during sample injection, *equilibrium* (if reached) during sample injection, where the rate of analyte binding is balanced with complex dissociation, and *dissociation* of analyte-ligand complex due to buffer flow immediately

after the end of analyte injection. With suitable analysis of binding data, reliable affinity and kinetic data can be obtained from SPR experiments. However, for the majority of experimental purposes, semi-quantitative ranking of rates and/or affinities is sufficient.

0.3.1 Basic theory[3,31,37,55,56]

A 1:1 interaction between the analyte (A) continuously flowing in solution over the ligand (B) surface may be described by:

$$A + B \underset{k_d}{\overset{k_a}{\rightleftharpoons}} AB$$
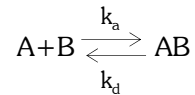
Considering that, in the *association phase*, the sensor surface is continuously replenished with free analyte solution and the amount of bound analyte is negligible with respect to the total analyte concentration (C), pseudo-first order kinetics can be assumed. Thus, the rate of complex formation is given by the equation:

$$d[AB]/dt = k_a[A][B] - k_d[AB] \qquad (0.7)$$

which, in terms of SPR response, can be expressed as:

$$dR/dt = k_a C(R_{max} - R) - k_d R = k_a C R_{max} - (k_a C + k_d)R \qquad (0.8)$$

where:

- R is the SPR response (in resonance units, RU) at time t;
- R_{max} is the maximum analyte binding capacity (in RU), which reflects the number of ligand binding sites, *i.e.*, total ligand concentration;
- k_a is the association rate constant;
- k_d is the dissociation rate constant.

Therefore, a plot of dR/dt against R will be a straight line of slope $-(k_a C + k_d)$ or $-k_s$, where k_s is the apparent binding rate, and a plot of k_s against analyte concentration will give a straight line with slope k_a and intercept on the ordinate k_d.

When *equilibrium* is reached, the total binding rate (dR/dt) is zero and, from equation 0.8:

$$k_a C(R_{max} - R_{eq}) = k_d R_{eq} \qquad (0.9)$$

Where R_{eq} is the total response at equilibrium. Considering that the *affinity* association constant (K_A) is given by k_a/k_d, binding affinity can be determined from equilibrium measurements, as it can be inferred from substituting and rearranging equation 0.9:

$$R_{eq}/C = K_A R_{max} - K_A R_{eq} \qquad (0.10)$$

Thus, by plotting R_{eq}/C against R_{eq}, a straight line is obtained and K_A and R_{max} can be calculated from the slope and the intercept on the ordinate, respectively.

During the *dissociation phase*, analyte solution is replaced by a continuous flow of running buffer solution and analyte concentration drops to zero. For the pseudo-first order kinetics model, complex dissociation can be described by:

$$dR/dt = -k_d R \qquad (0.11)$$

which, in the logarithmic form, can be given by:

$$ln(R_0/R_t) = k_d(t-t_0) \qquad (0.12)$$

where R_0 is the response at an arbitrary start dissociation time t_0. Consequently, a plot of $ln(R_t/R_0)$ will give a straight line with slope $-k_d$.

This basic theoretical model only applies when the interaction is homogeneous and when the pseudo-first order kinetics is actually observed.

0.3.2 Fitting and evaluating biosensor data[55-58]

Curve fitting methods

In early kinetic studies based on SPR biospecific interaction analysis, data evaluation relied upon *linearisation* of the binding data, according to the equations described in the previous section. Nevertheless, linear transformations also transform the parameter-associated errors, which decreases the quality of primary data.

On the other hand, it requires data from many analyte concentrations. Therefore, *non-linear least squares analysis* has been introduced for fitting and evaluating biosensor data[57]. Non-linear least squares methods optimise parameter values by minimising the sum of the squared residuals (S), being the latter the difference between the fitted (r_f) and the experimental (r_x) curves at each point (residuals are squared in order to equal the weight of deviations above and below the experimental curve, Fig. 0.14, Eq. 0.13).
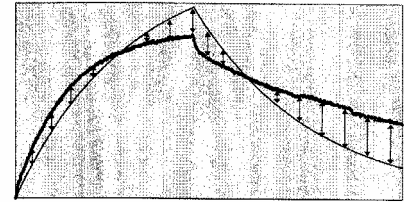

Figure 0. 14 Schematic representation of non-linear least squares fitting by minimising squared residuals[55].

$$S = \sum_1^n \left(r_f - r_x \right)^2 \qquad (0.13)$$

Non-linear least squares analysis has been applied to curve fitting based on the *integrated rate equations* (Table 0.2, page 21). This *analytical integration* is the simplest tool for systems with rate equations that can be readily integrated. However, many interactions studied on biosensors do not fit simple kinetic models, which can be seen by curved plots when linearisation is applied or by poor fits when using the integrated rate equations. The software currently employed for biosensor data evaluation includes several kinetic fitting models (Table 0.2, page 21). Those models corresponding to binding that can be described by well-known rate equations use analytical integration while more complex models, such as interactions with mass transfer limitations or conformational changes, rely upon curve fitting with *numerical integration*[58]. Numerical integration is more computationally-intensive but allows evaluation when the rate equations cannot be integrated analytically. In numerical integration methods, each species is assigned an initial concentration and the reaction is stepped through in discrete time intervals. At the end of each interval the concentration of each species is calculated considering its rate of formation or disappearance according to the rate equations. Numerical integration can be used to model any kinetic mechanism and also to analyse biosensor data by curve fitting as is done with analytical integration. However, with numerical methods data is usually analysed globally by fitting both the association and dissociation phases for several concentrations simultaneously. *Global curve fitting* is advantageous, because it minimises the possibility of having a good fit with a wrong kinetic model and it lowers the variance in the estimates of the rate constants.

Evaluating fitted data

The fitting algorithms are purely mathematical tools without any biochemical "knowledge". Therefore, it is always important to examine the results of fitted data to check for "reasonableness" of the parameters found. This must be kept in mind at the time of choosing the "best fit". This best fit depends on the ability of the fitting algorithm to converge for the true minimum in the sum of squared residuals and on the number of parameters that can be varied in the model, *i.e.*, the complexity of the model. Increasing model complexity also increases the probability to fall in local minima and obtain misleading fits. Wrong fits are usually evident from markedly poor curve fits or unreasonable results and are often due to bad data quality or inadequate choice of the fitting model. Increasing the complexity of a model will also increase the ability of fitting the experimental curves to the equation, since there is a wider range for varying parameters in order to obtain a closer fit. Therefore, it is important to accept the simplest model that fits the sensorgrams when evaluating kinetic data and judge whether a slightly better fit with a more complex model is experimentally significant. The quality of the fit is described by the *chi* squared statistical parameter, defined as:

$$\chi^2 = S/(n\text{-}p) \qquad\qquad (0.14)$$

where n is the number of data points, p is the number of fitted parameters and S is the sum of the residuals (Eq. 0.13). Since $n >> p$, χ^2 reflects the average squared residual *per* data point and, when

the model fully fits the experimental data, χ^2 represents the mean square of the signal noise. In practice it is useful to check for the shape of the residual plot, since non-random distribution of residuals is often a symptom of an incorrect fit.

0.3.3   Deviations from the langmuirian behaviour[2,3,37,51,55,58-72]

a) Mass-transport limitations[2,3,51,55,59-66]

Transport of mobile analyte to the sensor surface (Fig. 0.15) may be a serious problem when the interaction is fast. Insufficient transport rate will not allow to obtain meaningful kinetics (the rate-limiting step will be the diffusion into the dextran matrix and not the interaction itself) and the assumption that analyte bulk concentration is constant and equal to the injected concentration is no longer valid. Consequently, the rate equations corresponding to pseudo-first-order kinetics

Figure 0. 15 Scheme of the different factors influencing transport of mobile analyte to the sensor surface with immobilised ligand[2].

are not applicable to systems under diffusion-controlled kinetics. Diffusion effects can be minimised using high flow rates (> 30 μl/min), low density ligand surfaces and high analyte concentrations. Nevertheless, systems with very high interaction rates will be always diffusion-controlled, which implies an upper limit to the range of association rate constants amenable to study by SPR. Another effect related to mass-transport limitations is analyte *rebinding* during the dissociation phase. If analyte depletion from the surface is not fast enough, analyte molecules will rebind to the ligand and response no longer follows a single exponential decay.
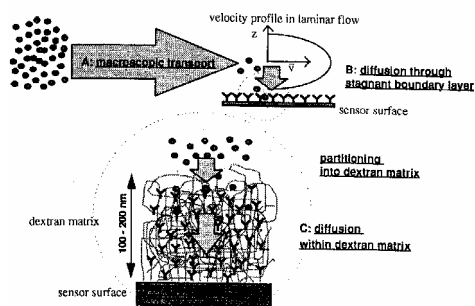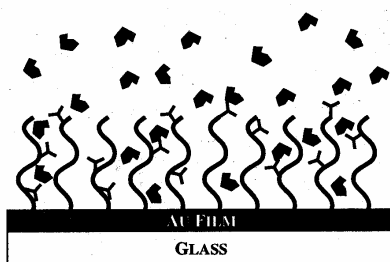

Figure 0. 16 Illustration of heterogeneous binding of analyte to ligand molecules immobilised in exposed and buried sites[59].

b) Ligand heterogeneity[2,3,55,58-61,67,68]

Random immobilisation chemistries and high surface density lead to heterogeinety of ligand sites, which therefore are no longer equivalent neither independent (Fig. 0.16). This effect is more pronounced with high analyte concentrations, *i.e.*, with decreasing number of free "readily accessible⇔higher affinity" ligand sites. Oriented attachment of ligand to the dextran layer, low analyte concentrations and low immobilisation levels are the best measures to avoid heterogeneity effects.

c) Analyte heterogeneity[3,55,59]

Although biospecific analysis allows for the utilisation of non-purified samples (concentration measurements of bioactive molecules in biological samples, ligand fishing, etc.), it must be ensured that samples for kinetic analysis do not contain molecules, other than the analyte, that can interact with the ligand. Otherwise, the SPR response will reflect the sum of different binding events and cannot be described by simple kinetics.
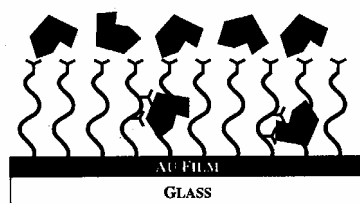
Figure 0. 17 Illustration of the parking problem: masking of ligand binding sites by attachment of large analyte molecules[59].

d) *Steric hindrance*[2,59,60]

The formation of a complex between a large analyte and immobilised ligand can mask additional binding sites. Although it could be argued that such steric hindrance would not affect binding kinetics (it would only decrease R_{max}), this is not strictly true, since the flexibility/fluidity of the dextran matrix allows temporarily masked sites to become accessible during analyte injection, adding complexity to the kinetics of the interaction. This problem, also named the *parking problem*, assumes greater proportions for large macromolecular analytes, higher analyte concentrations and high density ligand surfaces (Fig. 0.17).

e) *Analyte multivalency and ligand co-operativity*[51,55,59,69]

Poor fits with pseudo-first-order kinetics should be expected whenever analyte is multivalent (*e.g.* antibody bivalency), since 1:1 stoichiometry is no longer observed. Also, it is difficult to ensure that both analyte binding sites (in the case of bivalency) are equivalent and independent, as well as to know to which extent has the interaction 1:1 or 1:2 stoichiometry. Another situation where binding sites may not be independent occurs when there is ligand co-operativity. Although equivalent, the ligand binding sites may not interact independently from each other and negative or positive co-operative interactions will prevent the system from following simple pseudo-first-order kinetics.

f) *Conformational changes*[58-60]

It has been suggested that non-conformity of sensorgrams with the langmuirian model could be due to additional steps involving isomerisation of the AB complex. Such two-state-reactions, where there is conformational change upon binding, are not well described by pseudo-first-order kinetics and other models must be employed to fit the data.

0.3.4 Experimental design in kinetic SPR analysis[2,3,37,51,55,61,68-72]

Deviations to pseudo-first-order kinetics predicted for 1:1 interactions could be interpreted as due to more complex interaction mechanisms describing the interactions. However, they are often produced by artefacts which can be minimised by careful experimental design. *Low ligand immobilisation levels* are advisable to avoid mass-transport limitations, ligand heterogeneity or steric hindrance. *Analyte concentration* must be high enough to avoid diffusion-controlled kinetics and low enough not to saturate the surface (between $0.1K_D$ and $10 K_D$). *Buffer flow* must be kept at high rate to minimise diffusion-controlled binding and, whenever possible, soluble ligand must be added to buffer in the dissociation phase to avoid rebinding effects. *Oriented immobilisation chemistries* should be used when random amine coupling is seen to be a significative source of surface heterogeneities. *Instrumental drifts* or *non-specific binding* to the carboxymethyldextran matrix are often eliminated by subtraction of a blank run, using either an inactive analyte or a suitable reference cell with inactive ligand. If problems with non-specific binding are persistent, the choice of another kind of surface (other model of sensor chip) may be the solution.

Table 0.2 Rate equations used in the pre-defined fitting models included in the BIAevaluation 3.0 software[55].

Simultaneous k_a/k_d fit			
	Differential equations	**Total response**	**Reaction scheme**
(a) 1:1 langmuirian binding	$d[B]/dt=-(k_a[A][B]-k_d[AB])$ $d[AB]/dt=k_a[A][B]-k_d[AB]$	$[AB]+RI$	$A+B \Leftrightarrow AB$ $[A]=C$, $[B]_0=R_{max}$, $[AB]_0=0$
(b) 1:1 binding with drifting baseline	*the same as in (a)*	$[AB]+drift(t-t_{on})+RI$	*the same as in (a)*
(c) 1:1 binding with mass transfer	*the same as in (a) plus* $d[A]/dt=k_t(C-[A])-(k_a[A][B]-k_d[AB])$	$[AB]+RI$	$A_{bulk} \Leftrightarrow A+B \Leftrightarrow AB$ $[A]_{bulk}=C$, $[B]_0=R_{max}$, $[AB]_0=0$
(d) Heterogeneous ligand (2 different binding sites)	$d[B_1]/dt=-(k_{a1}[A][B_1]-k_{d1}[AB_1])$ $d[AB_1]/dt=k_{a1}[A][B_1]-k_{d1}[AB_1]$ $d[B_2]/dt=-(k_{a2}[A][B_2]-k_{d2}[AB_2])$ $d[AB_2]/dt=k_{a2}[A][B_2]-k_{d2}[AB_2]$	$[AB_1]+[AB_2]+RI$	$A+B_1 \Leftrightarrow AB_1$ $A+B_2 \Leftrightarrow AB_2$ $[A]=C$, $[B_1]_0=R_{max1}$, $[B_2]_0=R_{max2}$ $[AB_1]_0=[AB_2]_0=0$
(e) Heterogeneous analyte (competition between two different analytes)	$d[B]/dt=-(k_{a1}[A_1]mw_1[B]-$ $k_{d1}[A_1B])/mw_1n_1-(k_{a2}[A_2]mw_2[B]-$ $k_{d2}[A_2B])/mw_2n_2$ $d[A_1B]/dt=k_{a1}[A_1]mw_1[B]-k_{d1}[A_1B]$ $d[A_2B]/dt=k_{a2}[A_2]mw_2[B]-k_{d2}[A_2B]$	$[A_1B]+[A_2B]+RI$	$A_1+B \Leftrightarrow A_1B$ $A_2+B \Leftrightarrow A_2B$ $[A_1]=C_1$, $[A_2]=C_2$, $[B]_0=R_{max}/mw_1$, $[A_1B]_0=[A_2B]_0=0$
(f) Bivalent analyte	$d[B]/dt=-(k_{a1}[A][B]-k_{d1}[AB])-$ $(k_{a2}[AB][B]-k_{d2}[AB_2])$ $d[AB]/dt=(k_{a1}[A][B]-k_{d1}[AB])-$ $(k_{a2}[AB][B]-k_{d2}[AB_2])]$ $d[AB_2]/dt=k_{a2}[AB][B]-k_{d2}[AB_2]$	$[AB]+[AB_2]+RI$	$A+B \Leftrightarrow AB$ $AB+B \Leftrightarrow AB_2$ $[A]=C$, $[B]_0=R_{max}$, $[AB]_0=[AB_2]_0=0$
(g) Conformational change (two-state reaction)	$d[B]/dt=-(k_{a1}[A][B]-k_{d1}[AB])$ $d[AB]/dt=(k_{a1}[A][B]-k_{d1}[AB])-$ $(k_{a2}[AB]-k_{d2}[AB^*])$ $d[AB^*]/dt=k_{a2}[AB]-k_{d2}[AB^*]$	$[AB]+[AB^*]+RI$	$A+B \Leftrightarrow AB \Leftrightarrow AB^*$ $[A]=C$, $[B]_0=R_{max}$, $[AB]_0=[AB^*]_0=0$

Separate k_a/k_d fit			
	Integrated rate equations		
(h) 1:1 langmuirian binding	$R = \dfrac{Ck_a R_{max}\left[1-e^{-((Ck_a+k_d)t)}\right]}{Ck_a+k_d}+RI$ $R = R_0 e^{-k_d t}+offset$	$[AB]+RI$ $[AB]+offset$	*the same as in (a)*

References

1 Garland, P. B. (1996) Optical evanescent wave methods for the study of biomolecular interactions, *Quart. Rev. Biophys.* **2**, 91-117.

2 Schuck, P. (1997) Use of surface plasmon resonance to probe the equilibrium and dynamic aspects of interactions between biological macromolecules, *Annu. Rev. Biophys. Biomol. Struct.* **26**, 541-566.

3 "BIAcore Instrument Handbook", (Pharmacia Biosensor AB, 1994) Uppsala, Sweden.

4 Hirshcfield, T. (1967), Physics of Thin Films **9**, 145.

5 Kretschmann, E. and Raether, H. (1968) Radiative decay of non-radiative surface plasmons excited by light, *Z. Natuforsch.* **23A**, 2135-2136.

6 Homola, J., Yee, S. S. and Gauglitz, G. (1999) Surface plasmon resonance sensors: review, *Sens. & Actuat. B* **54**, 3-15.

7 Margheri, G., Mannoni, A. and Quercioli F. (1996) A new high-resolution displacement sensor based on surface plasmon resonance, *Proc. SPIE* **2783**, 211-220.

8 Schaller, J. K., Czepluch, R. and Stojanoff, C. G. (1997) Plasmon spectroscopy for high resolution angular measurements, *Proc. SPIE* **3098**, 476-486.

9 Weiss, M. N., Srivastava, R. and Groger, H. (1996) Experimental investigation of a surface plasmon-based integrated-optic humidity sensor, *Electron. Lett.* **32**, 842-843.

10 Chadwick, B. and Gal, M. (1993) An optical temperature sensor using surface plasmons, *Japn. J. Appl. Phys.* **32**, 2716-2717.

11 Miwa, S. and Arakawa, T. (1996) Selective gas detection by means of surface plasmon resonance sensors, *Thin Solid Films* **281-282**, 466-468.

12 Abdelghani, A., Chovelon, J. M., Jaffrezic-Renault, N., Ronot-Trioli C., Veillas, C. and Gagnaire, H. (1997) Surface plasmon resonance fiber-optic sensor for gas detection, *Sens. & Actuat. B* **38-39**, 407-410.

13 Podgorsek, R. P., Sterdenburgh, T. Wolters, J. Ehrenreich, T., Nischwitz, S. and Franke, H. (1997) Optical gas sensing by evaluating ATR leaky mode spectra, *Sens. & Actuat. B* **39**, 349-352.

14 Chadwick, B. and Gal, M. (1994) A hydrogen sensor based on the optical generation of surface plasmons in a palladium alloy, *Sens. & Actuat. B* **17**, 215-220.

15 Ashwell, G. J. and Roberts, M. P. S. (1996) Highly selective surface plasmon resonance sensor for NO_2, *Electron. Lett.* **32**, 2089-2091.

16 Granito, C., Wilde, J. N., Petty, M. C., Houston, S. and Iradale, P.J. (1996) Toluene vapor sensing using copper and nickel phthalocyanine Langmuir-Blodgett films, *Thin Solid Films* **284-285**, 98-101.

17 Van Gent, J., Lambeck, P. V., Bakker, R. J., Popma, T. J., Sudholter, E.J.R. and Reinhoudt, D.N. (1991) Design and realization of a surface plasmon resonance-based chemo-optical sensor, *Sens. & Actuat. A* **26**, 449-452.

18 Chinowsky, T. M., Saban, S. B. and Yee, S. S. (1996) Experimental data from a trace metal sensor combining surface plasmon resonance with anodic stripping voltammetry, *Sens. & Actuat. B* **35**, 37-43.

19 Liedberg, B., Nylander, C. and Lundström, K. (1983) Surface plasmons resonance for gas detection and biosensing, *Sens. & Actuat.* **4**, 299-304.

20 Johnsson, B., Löfås, S. and Lindquist, G. (1991) Immobilization of proteins to a carboxymethyldextran-modified gold surface for biospecific interaction analysis in surface plasmon resonance sensors, *Anal. Biochem.* **198**, 268-277.

21 Fägerstam, L. G., Frostel-Karlsson, Å., Karlsson, R., Persson, B. and Rönnberg, I. (1992) Biospecific interaction analysis using surface plasmon resonance detection applied to kinetic, binding site and concentration analysis, *J. Chrom.* **597**, 397-410.

22 http://www.biacore.com/

23 Altschuh, D., Dubs, M. C., Weiss, E., Zeder-Lutz, G. and Van Regenmortel, M. H. V. (1992) Determination of kinetic constants for the interaction between monoclonal antibody and peptides using surface plasmon resonance, *Biochemistry* **31**, 6298-6304.

24 Lasonder, E., Bloemhoff, W. and Welling, G. W. (1994) Interaction of lysozyme with synthetic anti-lysozyme D1.3 antibody fragments studied by affinity chromatography and surface plasmon resonance, *J. Chrom. A* **676**, 91-98.

25 Lasonder, E., Schellekens, G. A., Koedijk, D. G. A. M., Damhof, R. A., Welling-Wester S., Feijlbrrief, M., Scheffer, A. J. and Welling, G. W. (1996) Kinetic analysis of synthetic analogues of linear-epitope peptides of glycoprotein D of herpes simplex virus type I by surface plasmon resonance, *Eur. J. Biochem.* **240**, 209-214.

26 Houshmand, H., Fröman, G. and Magnusson, G. (1999) Use of bacteriophage T7 displayed peptides for determination of monoclonal antibody specificity and biosensor analysis of the binding reaction, *Anal. Biochem.* **268**, 363-370.

27 Wu, Z., Johnson, K., Choi, Y. and Ciardelli, T. L. (1995) Ligand binding analysis of soluble interleukin 2-receptor complexes by surface plasmon resonance, *J. Biol. Chem.* **270**, 16045-16051.

28 Lessard, I. A. D., Fuller, C. and Perham, R. N. (1996) Competitive interaction of component enzymes with the peripheral subunit-binding domain of the pyruvate-dehydrogenase multienzyme complex of *Baccilus stearothermophilus*: kinetic analysis using surface plasmon resonance detection, *Biochemistry* **35**, 16863-16870.

29 Cheskis, B. and Freedman, L. P. (1996) Modulation of nuclear receptor interactions by ligands: kinetic analysis using surface plasmon resonance, *Biochemistry* **35**, 3309-3318.

30 Dubs, M. C., Altschuh, D. and Van Regenmortel, M. H. V. (1992) Mapping of viral epitopes with conformationally specific monoclonal antibodies using biosensor technology, *J. Chrom.* **597**, 391-396.

31 Saunal, H. and Van Regenmortel, M. H. V. (1995) Mapping of viral conformational epitopes using biosensor measurements, *J. Immunol. Meth.* **183**, 33-41.

32 Hodgson, J. (1994) Light, Angles, Action: Instruments for label-free, real-time monitoring of intermolecular interactions, *Biotechnology* **12**, 31-35.

33 Malmqvist, M. and Karlsson, R. (1997) Biomolecular interaction analysis: affinity biosensor technologies for functional analysis of proteins, *Curr. Op. Chem. Biol.* **1**, 378-383.

34 Pathak, S. and Savelkoul, H. F. J. (1997) Biosensors in immunology: the story so far, *Immunol. Today* **18**, 464-467.

35 Fivash, M., Towler, E. M. and Fisher, R. J. (1998) BIAcore for macromolecular interaction, *Curr. Op. Biotechnol.* **9**, 97-101.

36 Lakey, J. H. and Raggett, E. M. (1998) Measuring protein-protein interactions, *Curr. Op. Struct. Biol.* **8**, 119-123.

37 "BIAapplications Handbook", (Pharmacia Biosensor AB, 1994) Uppsala, Sweden.

38 Sjölander, S. and Urbaniczky, C. (1991) Integrated fluid handling system for biomolecular interaction analysis, *Anal. Chem.* **63**, 2338-2345.

39 Löfås, S. and Johnsson, B. (1990) A novel hydrogel matrix on gold surfaces in surface plasmon resonance sensors for fast and efficient covalent immobilization of ligands, *J. Chem. Soc., Chem. Commun.*, 1526-1528.

40 O'Shannessy, D. J., Brigham-Burke, M. and Peck, K. (1992) Immobilization chemistries suitable for use in the BIAcore surface plasmon resonance detector, *Anal. Biochem.* **205**, 132-136.

41 Brigham-Burke, M., Edwards, J. R. and O'Shannessy, D. J. (1992) Detection of receptor-ligand interactions using surface plasmon resonance: model studies employing the HIV-1 gp120/CD4 interaction, *Anal. Biochem.* **205**, 125-131.

42 Lemmon. M. A., Ladbury, J. E., Mandiyan, V., Zhou, M. and Schlessinger, J. (1994) Independent binding of peptide ligands to the SH2 and SH3 domains of Grb2, *J. Biol. Chem.* **269**, 31653-31658.

43 Tamamura, H., Otaka, A., Murakami, T., Ishihara, T., Ibuka, T., Waki, M., Matsumoto, A., Yamamoto, N. and Fujii, N. (1996) Interaction of an anti-HIV peptide, T22, with gp120 and CD4, *Biochem. Biophys. Res. Comm.* **219**, 555-559.

44 Chao, H. Houston, M. E., Grothe, S., Kay, C. M., O'Connor-McCourt, M., Irvin, R. T. and Hodges, R. S. (1996) Kinetic study on the formation of a *de novo* designed heterodimeric coiled-coil: use of surface plasmon resonance to monitor the association and dissociation of polypeptide chains, *Biochemistry* **35**, 12175-12185.

45 England, P., Brégére, F. and Bedouelle, H. (1997) Energetic and kinetic contributions of contact residues of antibody D1.3 in the interaction with lysozyme, *Biochemistry* **36**, 164-172.

46 Huyer, G., Li, Z. M., Adam, M., Huckle, W. R. and Ramachandran, C. (1995) Direct determination of the sequence recognition requirements of the SH2 domains of SH-PTP2, *Biochemistry* **34**, 1040-1049.

47 Shen, B. J., Hage, T. and Sebald, W. (1996) Global and local determinants for the kinetics of interleukin-4/interleukin 4 receptor α chain interaction: a biosensor study employing recombinant interleukin-4 binding protein, *Eur. J. Biochem.* **240**, 252-261.

48 Lookene, A., Chevreuil, O., Østergaard, P. and Olivecrona, G. (1996) Interaction of lipoprotein lipase with heparin fragments and with heparan sulfate: stoichiometry, stabilization and kinetics, *Biochemistry* **35**, 12155-12163.

49 Van Regenmortel, M. H. V., Altschuh, D., Pellequer, J. L., Richalet-Sécordel, P., Saunal, H., Wiley, J. A. and Zeder-Lutz, G. (1994) Analysis of viral antigens using biosensor technology, *Methods: A Comp. Meth. Enzymol.* **6**, 177-197.

50 Zeder-Lutz, G., Rauffer, N., Altschuh, D. and Van Regenmortel, M. H. V. (1995) Analysis of cyclosporin interactions with antibodies and cyclophilin using BIAcore, *J. Immunol. Meth.* **183**, 131-140.

51 Nieba, L., Krebber, A. and Plükthun, A. (1996) Competition BIAcore for measuring true affinities: large differences from values determined from binding kinetics, *Anal. Biochem.* **234**, 155-165.

52 Karlsson, R. (1994) Real-time competitive kinetic analysis of interactions between low-molecular-weight ligands in solution and surface-immobilized receptors, *Anal. Biochem.* **221**, 142-151.

53 Andersson, K., Hamalainen, M. and Malmqvist, M. (1999) Identification and optimization of regeneration conditions for affinity-based biosensor assays. A multivariate cocktail approach, *Anal. Chem.* **71**, 2475-2481.

54 Andersson, K., Areskoug, D. and Hardenborg, E. (1999) Exploring buffer space for molecular interactions, *J. Molec. Recogn.* **12**,

55 "BIAevaluation Software Handbook: version 3.0", (Biosensor AB, 1997) Uppsala, Sweden.

56 Atkins P. W., "Physical Chemistry, 5th ed., Oxford University Press, Oxford, U. K. 1994.

57 O'Shannessy, D. J., Brigham-Burke, M., Soneson, K. K., Hensley, P. and Brooks, I. (1993) Determination of rate and equilibrium binding constants for macromolecular interactions using surface plasmon resonance: use of nonlinear least squares analysis methods, *Anal. Biochem.* **212**, 457-468.

58 Morton, T. A., Myszka, D. and Chaiken, I. (1995) Interpreting complex binding kinetics from optical biosensors: a comparison of analysis by linearization, the integrated rate equation and numerical integration, *Anal. Biochem.* **227**, 176-185.

59 O'Shannessy, D. J. and Winzor, D. J. (1996) Interpretation of deviations from pseudo-first-order kinetic behavior in the characterization of ligand binding by biosensor technology, *Anal. Biochem.* **236**, 275-283.

60 Bowles, M. R., Hall, D. R., Pond, S. M. and Winzor, D. J. (1997) Studies of protein interactions by biosensor technology: an alternative approach to the analysis of sensorgrams deviating from pseudo-first-order kinetic behavior, *Anal. Biochem.* **244**, 133-143.

61 Schuck, P. (1997) Reliable determination of binding affinity and kinetics using surface plasmon resonance biosensors, *Curr. Op. Biotech.* **8**, 498-502.

62 Glaser, R. W. (1993) Antigen-antibody binding and mass transport by convection and diffusion to a surface: a two-dimensional computer model of binding and dissociation kinetics, *Anal. Biochem.* **213**, 152-161.

63 Myszka, D., Arulanatham, P. R., Sana, T., Wu, Z., Morton, T. A. and Ciardelli, T. L. (1996) Kinetic analysis of ligand binding to interleukin-2 receptor complexes created on an optical biosensor surface, *Prot. Sci.* **5**, 2468-2478.

64 Hall, D. R., Cann, J. R. and Winzor, D. J. (1996) Demonstration of an upper limit to the range of association rate constants amenable to study by biosensor technology based on surface plasmon resonance, *Anal. Biochem.* **235**, 175-184.

65 Myszka, D., Morton, T. A., Doyle, M. L. and Chaiken, I. M. (1997) Kinetic analysis of a protein antigen-antibody interaction limited by mass transport on an optical biosensor, *Biophys. Chem.* **64**, 127-137.

66 Witz, J. (1999) Kinetic analysis of analyte binding by optical biosensors: hydrodynamic penetration of the analyte flow into the polymer matrix reduces the influence of mass transport, *Anal. Biochem.* **270**, 201-206.

67 Oddie, G. W., Gruen, L. C., Odgers, G. A., King, L. G. and Kortt, A. A. (1997) Identification and minimization of nonideal binding effects in BIAcore analysis: ferritin/anti-ferritin Fab' interaction as a model system, *Anal. Biochem.* **244**, 301-311.

68 Kortt, A. A., Oddie, G. W., Iliades, P., Gruen, L. C. and Hudson, P. J. (1997) Nonspecific amine immobilization of ligand can be a potential source of error in BIAcore binding experiments and may reduce binding affinities, *Anal. Biochem.* **253**, 103-111.

69 Kalinin, N. L., Ward, L. D. and Winzor, D. J. (1995) Effects of solute multivalence on the evaluation of binding constants by biosensor technology: studies with concanavalin A and interleukin-6 as partitioning proteins, *Anal. Biochem.* **228**, 238-244.

70 Catimel, B., Nerrie, M., Lee, F.T., Scott, A. M., Ritter, G., Welt, S., Old, L. J., Burgess, A. W. and Nice, E. C. (1997) Kinetic analysis of the interaction between the monoclonal antibody A33 and its colonic epithelial antigen by the use of an optical biosensor: a comparison of immobilisation strategies, *J. Chrom. A* **776**, 15-30.

71 Karlsson, R. and Fält, A. (1997) Experimental design for kinetic analysis of protein-protein interactions with surface plasmon resonance biosensors, *J. Immunol. Meth.* **200**, 121-133.

72 Ober, R. J. and Ward, E. S. (1999) The choice of the reference cell in the analysis of kinetic data using BIAcore, *Anal. Biochem.* **271**, 70-80.